Supporting Information

Direct comparison of covalently-linked dyad and a 1:1 mixture of tetrabenzoporphyrin and fullerene as organic photovoltaic materials

Yuto Tamura,[a] Hiroyuki Saeki,[a] Junpei Hashizume[b] Yukinori Okazaki,[b] Mitsuharu Suzuki,[a] Daiki Kuzuhara,[a] Naoki Aratani [a] and Hiroko Yamada [*ac]

[a]*Graduate School of Materials Science, Nara Institute of Science and Technology, 8916-5, Takayama-cho, Ikoma 630-0192, Japan, Fax: +81-743-72-6042; Tel: +81-743-72-6041;*

[b]*Graduate School of Science and Engineering, Ehime University, 2-5 Bunkyo-cho, Matsuyama, 790-8577, Japan;*

[c]*CREST, JST, 4-1-8 Honcho, Kawaguchi, Saitama 332-0012, Japan;*

Corresponding author E-mail: hyamada@ms.naist.jp

Contents

Experimental conditions

1. General

^{1}H NMR and ^{13}C NMR spectra were recorded on a JEOL JNM-ECX400 and AL 300 spectrometers at ambient temperature using tetramethylsilane as an internal standard. ESI and MALDI-TOF mass spectra were measured on a JEOL JMS-T100LC AccuTOF spectrometer and JEOL spiral TOF JMS-S3000 spectrometer, respectively. UV–vis spectra were measured on a JASCO UV/VIS/NIR Spectro-photometer V-570. Steady-state fluorescence spectra were measured on JASCO FP-6600 in the range of 400–800 nm. Fluorescence quantum yields were measured on an Absolute PL Quantum Yield Measurement System C9920-02. Thermogravimetric analysis were performed on a Seiko Thermal Analyser Exstar TG/DTA 6200.

2. Materials

Solvents and chemicals were reagent grade quality, obtained commercially and used without further purification except as noted. Thin-layer chromatography (TLC) and gravity column chromatography were performed on Art. 5554 (Merck KGaA), and Silica Gel 60N (Kanto Chemical Co.), respectively. For spectral measurements, spectral grade CH_2Cl_2 were purchased from Nacalai tesque Inc.

3. Cyclic voltammetry

CV measurements were conducted in a solution of 0.1 M $TBAPF_6$ in dry benzonitrile with a scan rate of 100 mV/s at room temperature in an argon-filled cell. A glassy carbon electrode and a Pt wire were used as a working and a counter electrode, respectively. An Ag/Ag^+ electrode was used as a reference electrode, which was normalized with the half-wave potential of ferrocene/ferrocenium$^+$ (Fc/Fc^+) redox couple.

4. Device fabrication and evaluation.

Indium-tin-oxide (ITO)-patterned glass substrates (20.0 × 25.0 mm, 15 Ω per square) were washed with running water and were ultrasonically cleaned in detergent, pure-water and isopropanol for 10 min each. After the substrates were dried, (3,4-ethylenedioxythiophene):poly(4-styrenesulfonate) (PEDOT:PSS, Clevios P VP AI4083, 200 μL) was spin coated at 3000 rpm for 30 s in air followed by a thermal annealing treatment at 130 °C for 10 min in air. The thickness of the resulting PEDOT:PSS layer was about 30 nm. The substrates were transferred to a N_2-filled glove box (<10 ppm O_2 and H_2O).

The deposition process of organic active layers is illustrated in Fig. S1. The p-layer was prepared by spin-coating of a chloroform solution (0.5 wt%, 100 μL, 2500 rpm, 30 s) of CP followed by heating (200 ºC, 20 min) to effect the in-situ conversion of **CP** to **BP**. The i (BHJ) layer for D–A compound was deposited in the similar manner with **CP–C_{60}** (0.7 wt%, 100 μL, 1500 rpm, 30 s) and heated (160 ºC, 20 min). For the reference i-layer, a mixed solution of CP and PCBM was spin-coated (0.7 wt%, 100 μL, 1500 rpm, 30 s) and heated (160 ºC, 20 min). The n-layer was prepared by spin-coating of a chloroform solution of $PC_{61}BM$ (0.5 wt%, 100 μL, 1500 rpm, 30 s) and annealed (195 ºC, 20 min). After preparation of the organic layers, aluminum (80 nm) was vapor deposited at high vacuum (5.0×10^{-5} Pa) through a shadow mask that defined an active area to 4.0 mm^2.

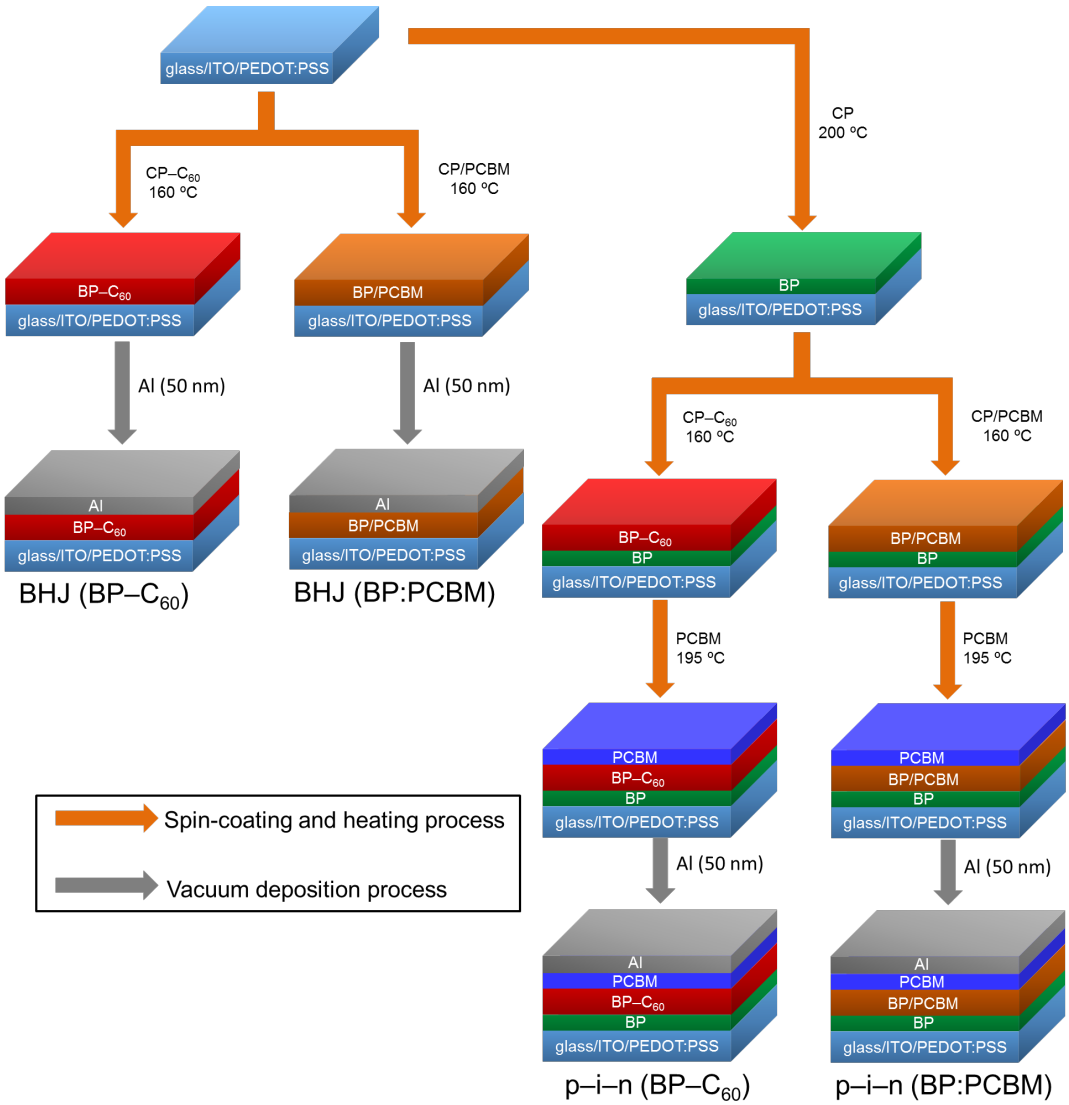

Fig. S1 Schematic description of fabrication procedure of the four different types of OPVs studied in this work. Typical concentration of the spin-coating solution is described.

Current–voltage (*J*–*V*) curves were measured using a Keithley 2611B SYSTEM Source Mater unit under AM1.5G illumination at an intensity of 100 mW cm^{-2} using a solar simulator (Bunko-keiki, CEP-2000RP). The external quantum efficiency (EQE) spectra were obtained under illumination of monochromatic light using the same system. The series resistance (R_s) and shunt resistance (R_{sh}) were obtained from light *J*-*V* curves.

5. Film characterization.

The film was prepared as described above on clean ITO glass without PEDOT:PSS. The surface morphology of organic films was observed by SPA400, SPI3800N AFM (Seiko instruments Inc.) in tapping mode using silicon probes with a resonant frequency of ~138 kHz and a force constant of 16 N m^{-1}. The bulk structure of thin-films was evaluated by out-of-plane X-ray diffraction (XRD) measurements using a RINT-TTRⅢ/NM diffractometer equipped with a rotating anode (Cu Kα radiation, λ = 1.5418 Å). Ionization potential of the films was measured by a Riken photoelectron spectroscopy instrument, AC-3.

Experimental section

1. Synthesis

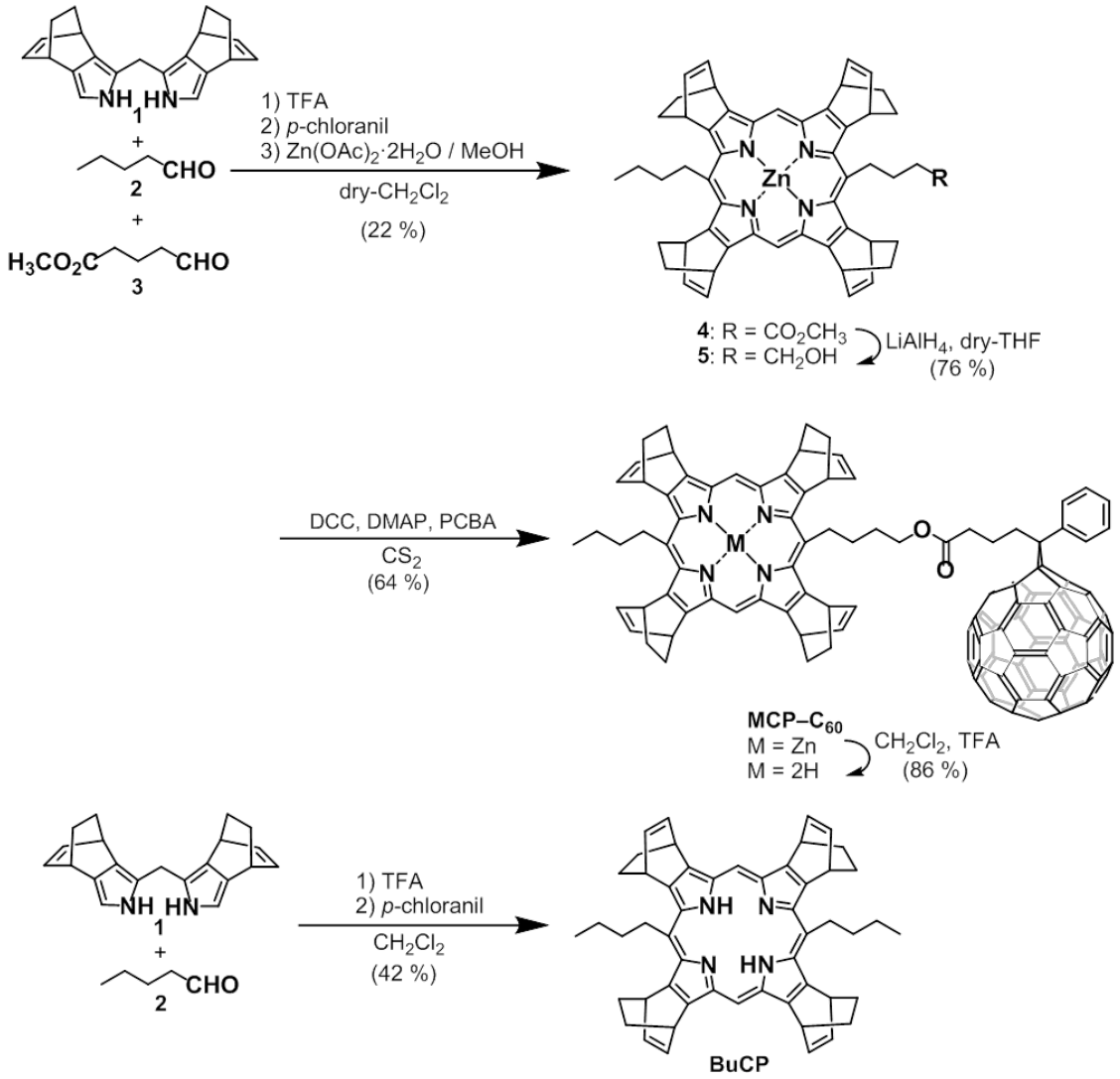

Scheme S1 Synthesis route of **CP–C_{60}** and **BuCP**

Porphyrin S4: S**1**[1] (1.04 g, 3.46 mmol), S**2** (86 mg, 1.04 mmol), and S**3**[2] (320 mg, 2.42 mmol) and dry-CH_2Cl_2 (600 mL) were added to a 1-L three-necked round-bottom flask under Ar. TFA (19 μm) was added to the solution, and the solution was stirred at room temperature for 16 h. After the addition of tetrachloro-*p*-benzoquinone (1.41 g, 5.75 mmol), the solution was stirred at room temperature for 2.5 h and was neutralized with triethylamine (1 mL). The solution was concentrated to 100 mL, and $Zn(OAc)_2 \cdot 2H_2O$(380 mg, 2.07 mmol) in methanol was added to the solution. The solution was stirred at room temperature for 3h. The solvent was removed by evaporation and the crude product was purified by silica gel column chromatography with ethyl

acetate/hexane (1:6) as an eluent to afford the purple powder S**4** (320 mg, 22%).

^{1}H NMR ($CDCl_3$, 400 MHz), δ: 10.15–10.33 (m, 2H), 7.06–7.23 (m, 8H), 5.06–5.85 (8H), 5.13–5.53 (m, 4H), 3.28–3.90 (m, 2H), 2.59–3.28 (m, 4H), 1.77–2.32 (m, 18H), 1.24–1.41 (m, 3H).

^{13}C NMR ($CDCl_3$, 100 MHz), δ: 173.92, 173.86, 151.46, 151.34, 148.02, 147.65, 143.87, 143.77, 140.50, 136.98, 120.40, 120.23, 118.35, 118.16, 96.61, 95.87, 52.12, 51.75, 41.38, 41.20, 40.92, 40.05, 36.00, 34.57, 33.87, 33.66, 33.37, 33.00, 32.61, 28.16, 27.66, 27.58, 27.46, 27.07, 23.81, 14.83, 14.69.

HR-MS (ESI): calcd for $C_{53}H_{53}N_4O_2Zn$, 841.3460 $[M + H]^+$; found, 841.3454.

Porphyrin S5: Porphyrin S4 (400 mg, 0.48 mmol) and dry-THF (12 mL) were added to a 50-mL two-necked round-bottom flask under N_2. $LiAlH_4$ (36 mg, 0.96 mmol) was added to the solution slowly, and stirred at room temperature for 12 h. A saturated aqueous solution of potassium sodium tartrate was added and the organic layer was extracted with ethyl acetate and washed with water and brine. The organic layer was dried over Na_2SO_4 and the solvent was removed by evaporation and the crude product was purified by silica gel column chromatography with ethyl acetate/hexanes (1:4) as an eluent and recrystallization from $CHCl_3$/hexanes to afford the pink powder S**5** (220 mg, 72%).

^{1}H NMR ($CDCl_3$, 400 MHz), δ: 10.14 (s, 2H), 7.04–7.22 (m, 8H), 5.69–5.82 (m, 8H), 5.17–5.47 (m, 4H), 3.79–4.04 (m, 2H), 2.64–3.06 (m, 4H), 1.80–2.51 (m, 20H), 1.22–1.46 (m, 4H).

^{13}C NMR ($CDCl_3$, 100 MHz), δ: 151.34, 151.33, 148.01, 147.75, 143.90, 143.78, 140.58, 140.51, 137.21, 137.15, 137.06, 120.26, 119.51, 119.37, 96.62, 96.54, 63.11, 40.96, 36.04, 34.53, 33.48, 31.60, 28.30, 28.27, 28.22, 28.18, 27.69, 27.66, 27.61, 27.59, 27.55, 27.51, 27.47, 27.11, 23.85, 22.66, 14.86, 14.14.

HR-MS (ESI): calcd for $C_{52}H_{53}N_4O_2Zn$, 813.3511 $[M + H]^+$; found, 813.3509.

ZnCP-C$_{60}$: Porphyrin S**5** (250 mg, 0.31mmol), PCBA[3] (330 mg, 0.37 mmol), *N,N'*-dicyclohexylcarbodiimide (DCC) (95 mg, 0.47 mmol), *N,N*-dimethyl-4-aminopyridine (DMAP) (4 mg, 0.03 mmol), and CS_2 (5 mL) were added to a 20-mL round-bottom flask. The reaction mixture was stirred at room temperature for 48 h. The solvent was removed by evaporation and the residue was purified by silica gel column chromatography with CH_2Cl_2 as an eluent and by GPC with $CHCl_3$ as eluent to afford the dark purple solid **ZnCP-C$_{60}$** (338 mg, 64%).

^{1}H NMR ($CDCl_3$, 400 MHz): δ: 10.06–10.23 (m, 2H), 7.32–7.68 (m, 5H), 6.94–7.24 (m, 8H), 5.60–5.86 (m, 8H), 5.16–5.54 (m, 4H), 4.25–4.45 (m, 2H), 1.56–3.00 (m, 30H), 1.29–1.45 (m, 3H).

^{13}C NMR ($CDCl_3$, 100 MHz), δ: 173.40, 173.26, 151.44–150.80,* 148.13–135.65,* 131.86, 131.75, 128.06, 127.93, 120.81, 120.61, 119.42, 119.37, 96.83, 96.70, 78.56, 78.35, 78.22, 78.18, 78.15, 65.67, 65.19, 65.07, 50.34, 41.13, 36.02, 35.97, 35.76, 34.16, 33.76, 32.84, 32.62, 32.41, 29.41, 28.78, 28.75, 28.53, 28.35, 27.73, 27.57, 27.41, 27.36, 23.78, 22.43, 14.96. *Overlapped broad peaks are observed presumably owing to intra or intermolecular interactions between the C_{60} core and the porphyrin unit, associated with the existence of multiple isomers depending on the orientation of bicyclo[2.2.2]octadieno-units.

HR-MS (ESI): calcd for $C_{123}H_{63}N_4O_2Zn$, 1691.4243 $[M + H]^+$; found, 1691.4253.

CP-C$_{60}$: **ZnCP-C$_{60}$** (300 mg, 0.18 mmol) and CH_2Cl_2 (25 mL) was added to a 50-mL round-bottom flask. TFA (67 μL, 0.88 mmol) was added to the solution, and stirred overnight at room temperature. The solution was washed with a saturated aqueous solution of $NaHCO_3$, water, and brine. The solvent was removed by evaporation and the crude product was purified by GPC with $CHCl_3$ as an eluent to afford the dark purple solid **CP-C$_{60}$** (260 mg, 89%).

^{1}H NMR ($CDCl_3$, 400 MHz), δ: 10.12–10.26 (m, 2H), 7.31–7.67 (m, 5H), 6.93–7.24 (m, 8H), 5.56–5.87 (m, 8H), 5.05–5.44 (m, 4H), 4.25–4.46 (m, 2H), 1.58–2.90 (m, 30H), 1.23–1.43 (m, 3H), -3.43–-3.11 (m, 2H).

^{13}C NMR ($CDCl_3$, 100 MHz), δ: 173.43, 173.28, 151.46–150.83,* 146.20–135.68,* 131.89, 131.79, 128.07, 127.97, 127.90, 119.76, 119.68, 119.63, 118.24, 118.14, 96.41, 96.14, 78.60, 78.40, 78.27, 65.64, 65.26, 65.15, 64.43, 50.24, 40.68, 40.20, 40.12, 36.06, 35.55, 35.37, 34.32, 33.28, 33.13, 32.93, 32.73, 32.58, 29.62, 29.58, 28.57, 28.39, 27.65, 27.49, 25.34, 23.85, 22.42, 22.28, 14.82. *Overlapped broad peaks are observed presumably owing to intra or intermolecular interactions between the C_{60} core and the porphyrin unit, associated with the existence of multiple isomers depending on the orientation of bicyclo[2.2.2]octadieno-units.

HR-MS (ESI): calcd for $C_{123}H_{65}N_4O_2$, 1629.5108 $[M+H]^+$; found, 1629.5094.

BuCP: S**1** (1.04 g, 3.46 mmol), S**2** (286 mg, 3.46 mmol) and dry-CH_2Cl_2 (600 mL) were added to a 1-L three-neck round-bottom flask under Ar. TFA (19 μl) was added and the solution was stirred at room temperature for 16 h. After the addition of tetrachloro-*p*-benzoquinone (1.41 g, 5.75 mmol), the solution was stirred at room temperature for 2.5 h and neutralized with

triethylamine (1 mL). The solvent was removed by evaporation and the crude product was purified by silica gel column chromatography with ethyl acetate/hexanes (1:6) as an eluent and recrystallization $CHCl_3$/MeOH to afford the purple powder **BuCP** (534 mg, 42%).

^{1}H NMR ($CDCl_3$, 400 MHz), δ: 10.15–10.33 (m, 2H), 7.04–7.22 (m, 8H), 5.66–5.85 (m, 8H), 5.11–5.37 (m, 4H), 2.58–2.86 (m, 4H), 1.76–2.30 (m, 20H), 1.21–1.40 (m, 6H), -3.13 (s, 2H).

^{13}C NMR ($CDCl_3$, 100 MHz), δ: 151.17, 151.15, 151.11, 146.07, 146.05, 141.31, 141.22, 136.84, 135.72, 135.70, 134.48, 119.01, 95.71, 95.68, 40.69, 40.10, 36.10, 33.20, 28.01, 27.50, 27.15, 23.78, 14.73.

HR-MS (ESI): calcd for $C_{52}H_{55}N_4$, 735.4427 $[M + H]^+$; found, 735.4418.

Thermal conversion of CP–C_{60} and BuCP to BP–C_{60} and BuBP was carried out at 200 °C for 1 h in vacuum. Because of their terribly low solubility, BP–C_{60} and BuBP were identified by thermal gravimetric analysis (Figs. S2 and S4) and MALDI-TOF mass spectrum (Figs. S3 and S5).

2. Thermal reaction profiles.

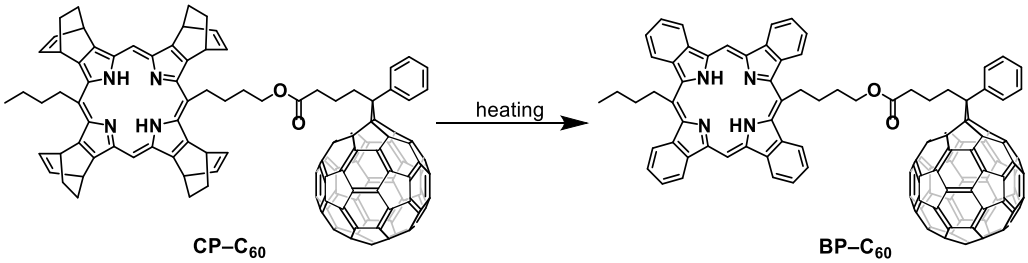

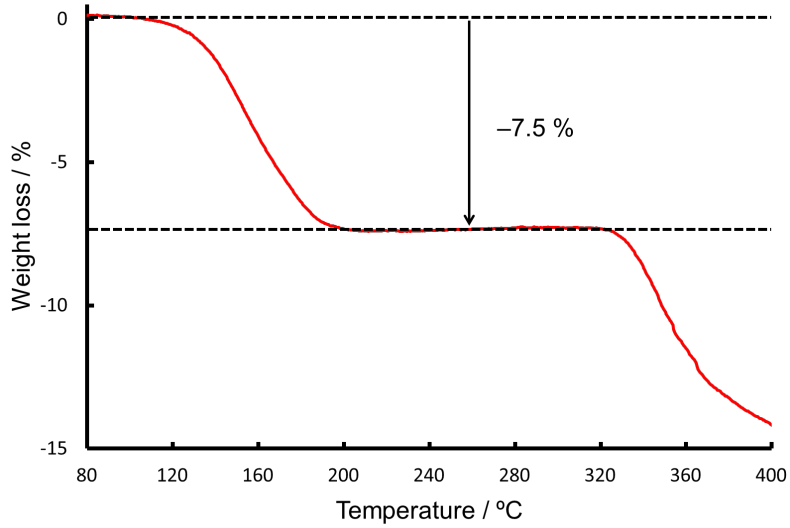

Fig. S2 Thermal gravimetric analysis of **CP–C$_{60}$**. The weight loss from 150 to 220 ºC was due to the release of four ethylene molecules from **CP–C$_{60}$**. The observed value was 7.5% and the calculated was 6.9%.

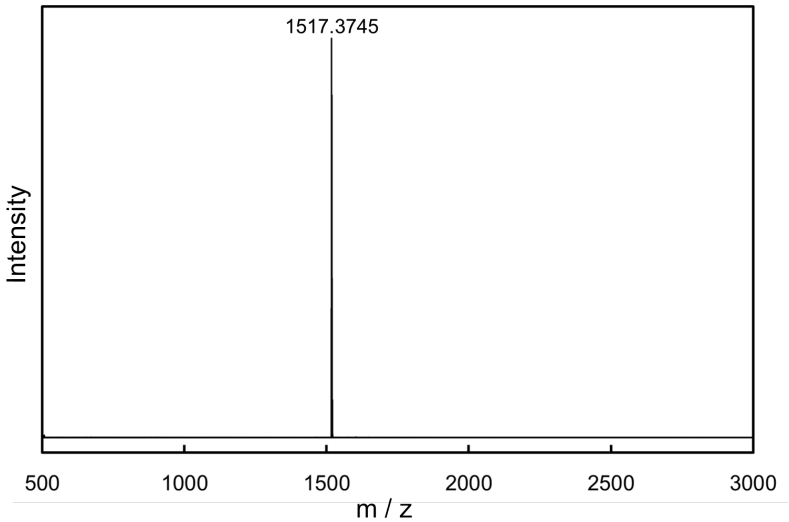

Fig. S3 MALDI-TOF mass spectrum after thermal reaction of **CP–C$_{60}$**.

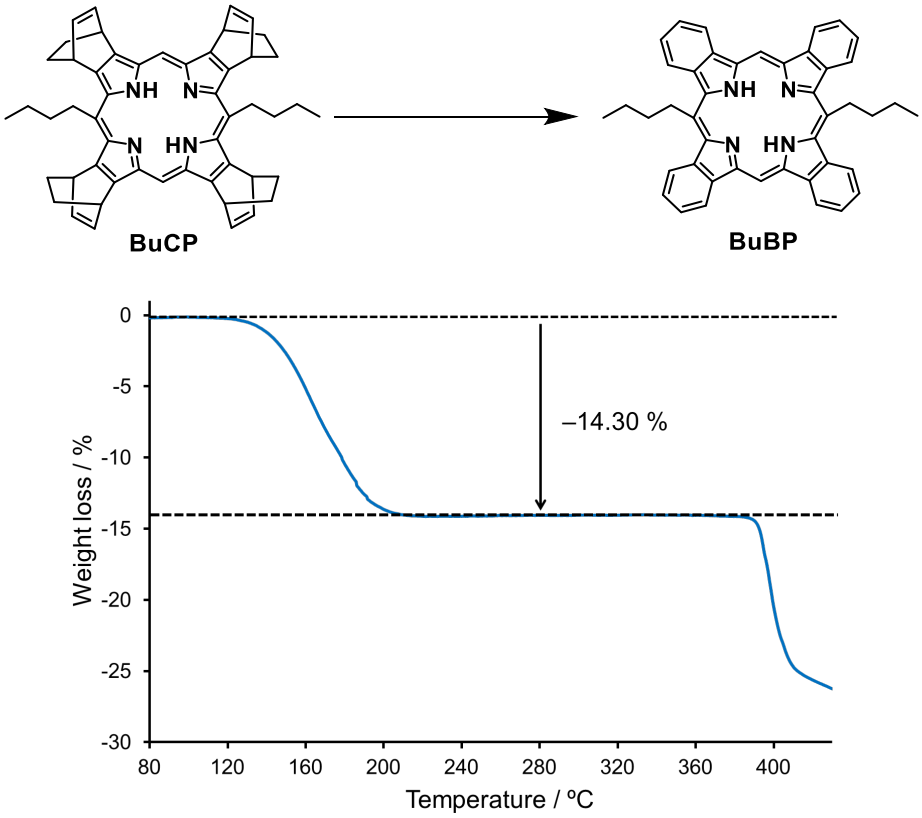

Fig. S4 Thermal gravimetric analysis of **BuCP**. The weight loss from 150 to 220 ºC was due to the release of four ethylene molecules from **BuCP**. The observed value was 14.30%, and the calculated was 15.27%.

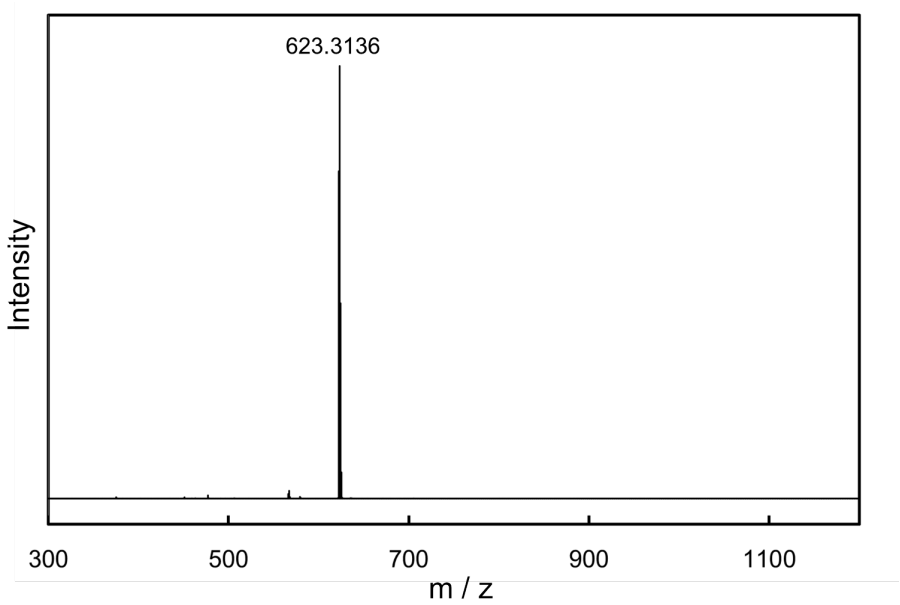

Fig. S5 MALDI-TOF mass spectrum after thermal reaction of **BuCP**.

3. UV–vis absorption spectra and fluorescence spectra

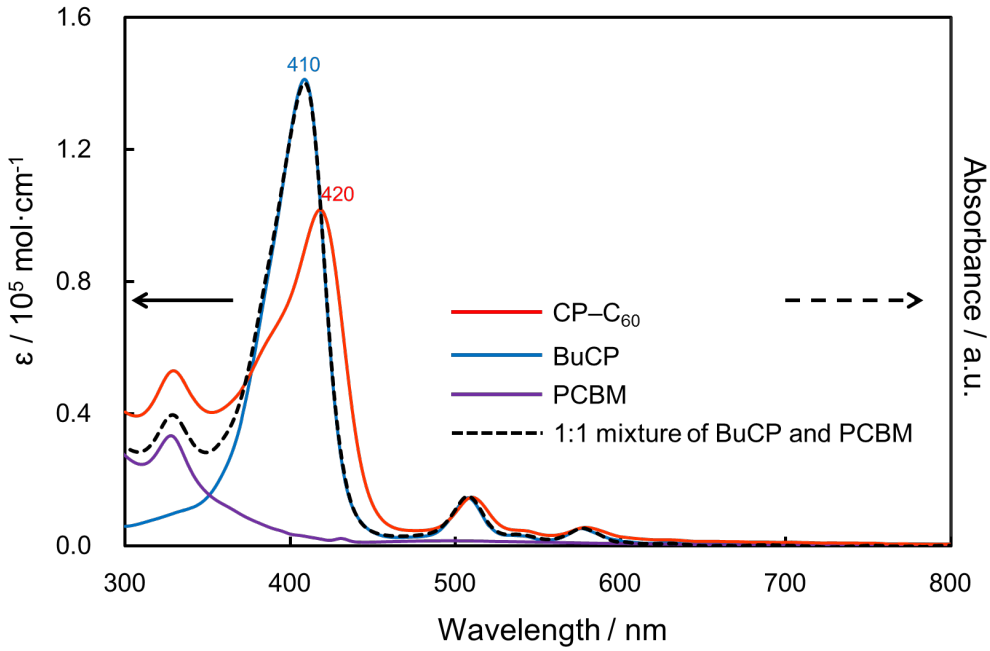

Fig. S6 The UV–vis absorption spectra of **CP–C$_{60}$**, **BuCP**, **PCBM** and a 1:1 mixture of **BuCP** and **PCBM** in CH_2Cl_2.

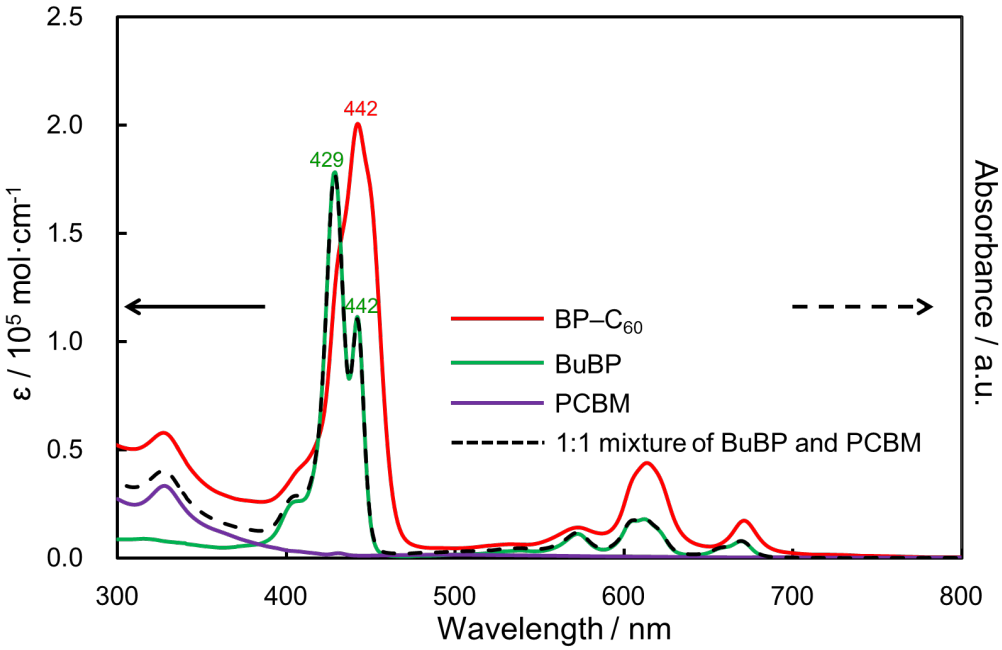

Fig. S7 UV–vis absorption spectra of **BP–C$_{60}$**, **BuBP**, **PCBM** and a 1:1 mixture of **BuBP** and **PCBM** in CH_2Cl_2.

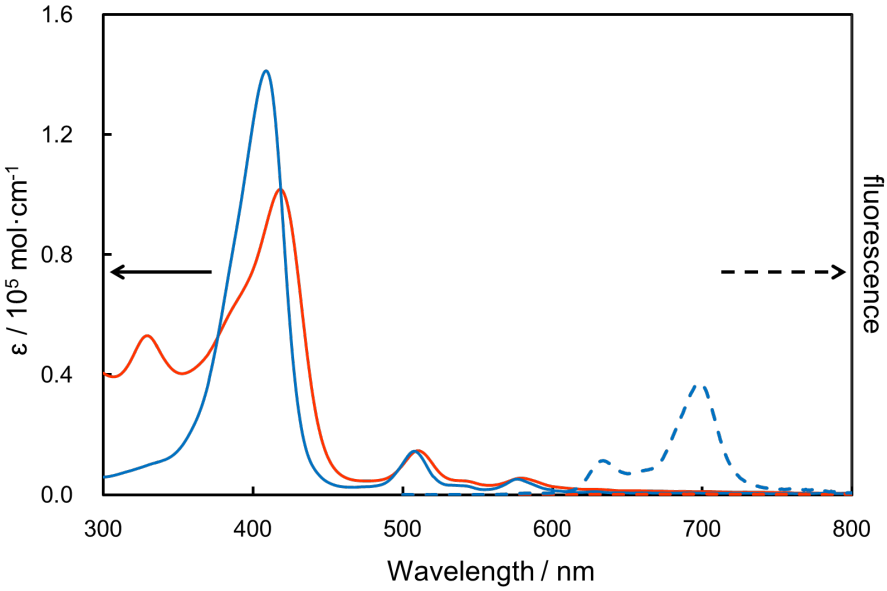

Fig. S8 The UV–vis absorption (solid lines) and fluorescence spectra (broken lines) of **BuCP** (blue lines) and **CP–C$_{60}$** (orange lines) in CH_2Cl_2.

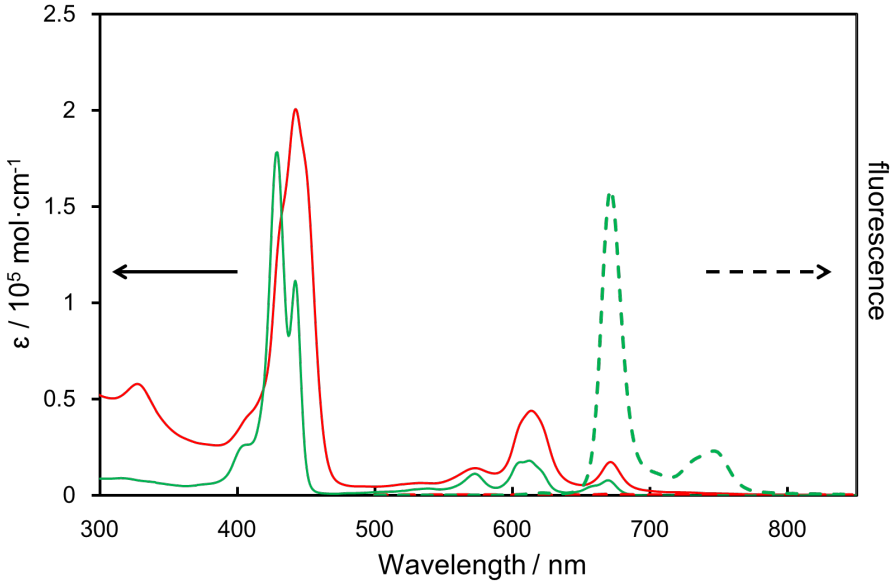

Fig. S9 The UV–vis absorption (solid lines) and fluorescence spectra (broken lines) of **BuBP** (green lines) and **BP–C$_{60}$** (red lines) in CH_2Cl_2.

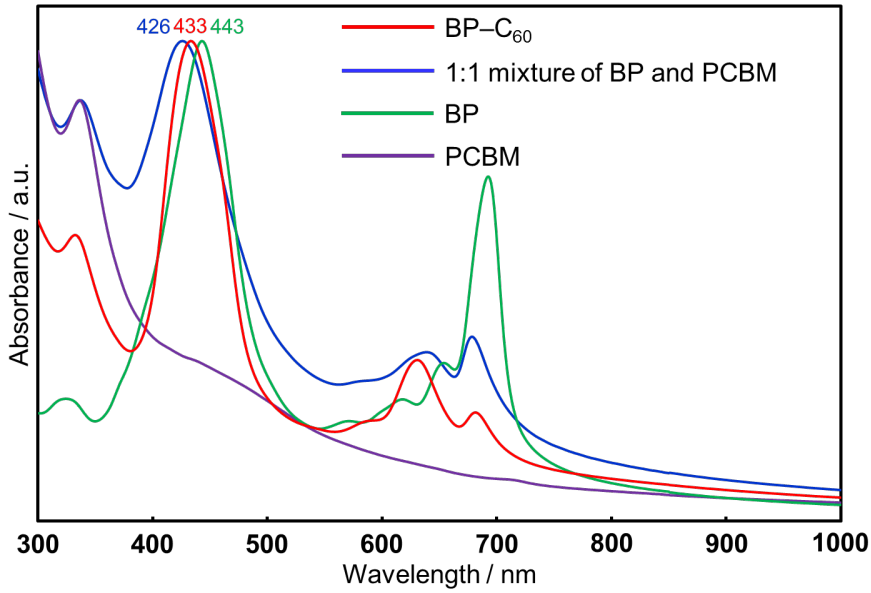

Fig. S10 Normalized UV–vis absorption spectra of **BP–C_{60}**, **BP**/**PCBM** (1:1 mol/mol) blend, **BP**, and **PCBM** as film.

4. Ionization potential

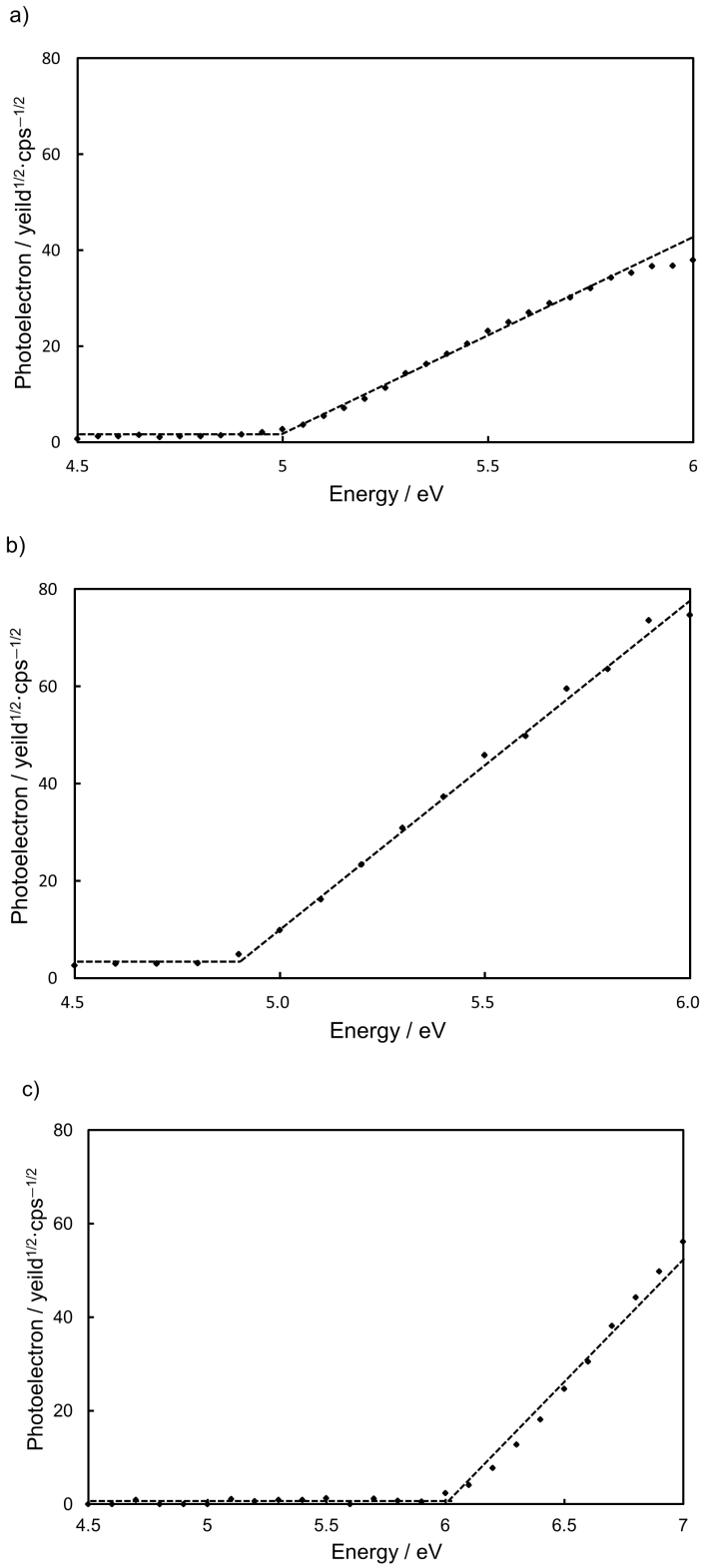

Fig. S11 Measurement of ionization potential of a) **BP–C_{60}**, b) **BP** and c) **PCBM**, films by photoelectron spectroscopy, AC–3. Broken lines are fitting lines.

5. Cyclic voltammetry

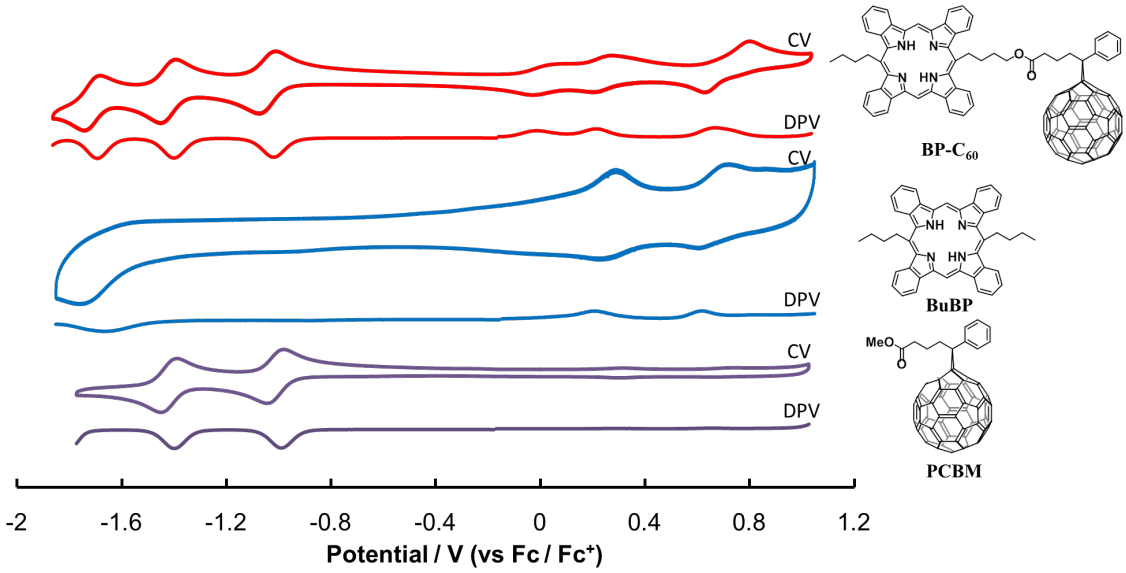

Fig. S12 a) Cyclic voltammograms (CVs) and differential pulse voltammograms (DPVs) of **BP–C$_{60}$** (red), **BuBP** (blue) and **PCBM** (purple) in benzonitrile.

Table. S1 HOMO and LUMO energy level of the materials for OPV

	E_{gap} [a] [eV]	$E_{1/2}^{ox}$ [b] [V]	$E_{1/2}^{red}$ [b] [V]	HOMO [c] [eV]	HOMO [d] [eV]	LUMO [e] [eV]	LUMO [f] [eV]
BP-C$_{60}$	1.6	—	−0.88	−5.0	−4.7	−3.4	−3.9
BP	1.7	—	—	−4.9	—	−3.2	—
BuBP	—	0.2	−1.7	—	−4.6	—	−3.1
PCBM	1.8	—	−1.0	−6.0	—	−4.2	−3.8

[a]Determined by absorption edge of the film; [b]Determined from the oxidation and reduction peaks obtained by cyclic voltammetry, V vs Fc/Fc$^+$; [c]Determined by photoemission yield spectroscopy in air; [d]HOMO = −(4.8 + $E_{1/2}^{ox}$); [e]Estimated from = E_{gap} and HOMO levels. LUMO = E_{gap} + HOMO; [f]LUMO = −(4.8 + $E_{1/2}^{red}$)

6. Current–voltage measurement

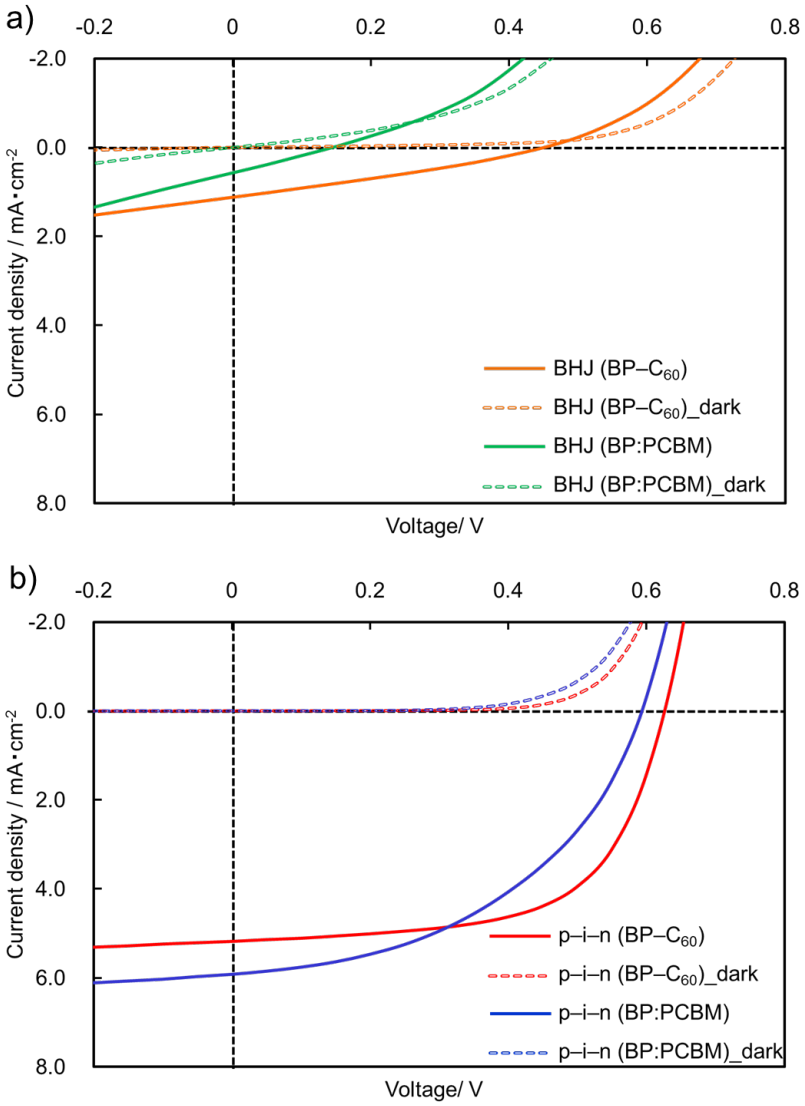

Fig. S13 The light and dark *J–V* characteristics of a) BHJ devices and b) p–i–n devices.

7. AFM

a)

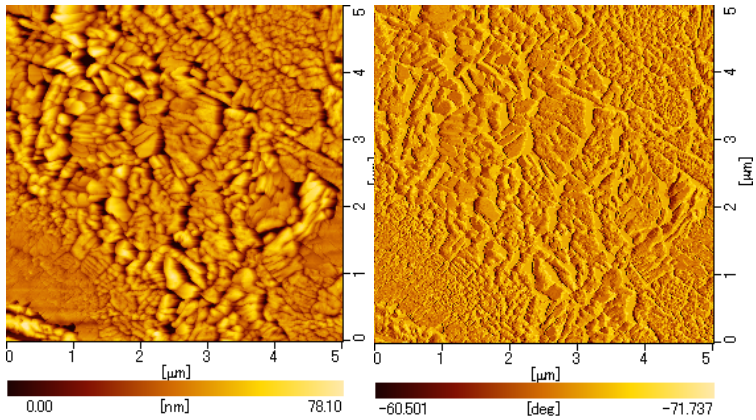

b)

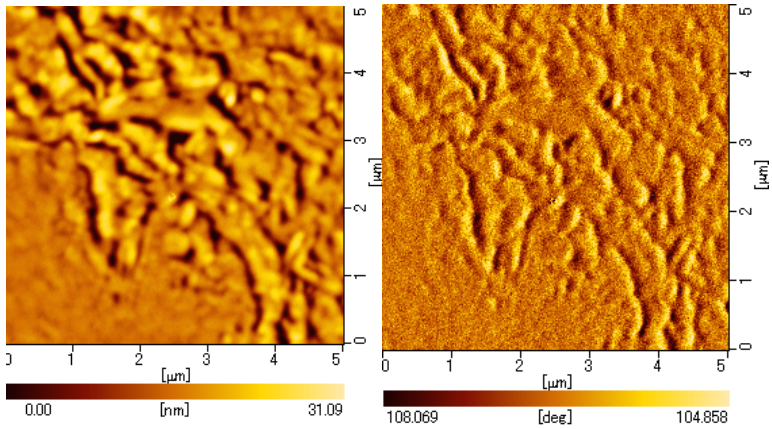

c)

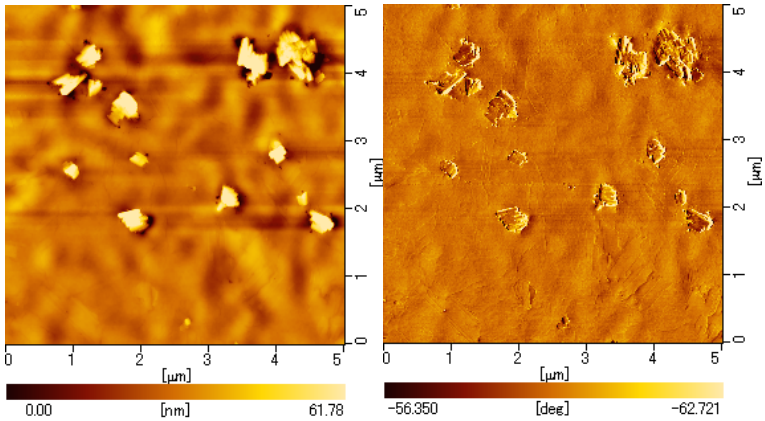

Fig. S14 Tapping–mode AFM height (left) and phase (right) images of a) **BP**-layer, b) **BP–C_{60}** -layer on **BP** layer and c) a mixed **BP:PCBM**-layer on **BP** layer. RMS values are 12.4, 4.88 and 8.83 nm for a), b), and c).

a)

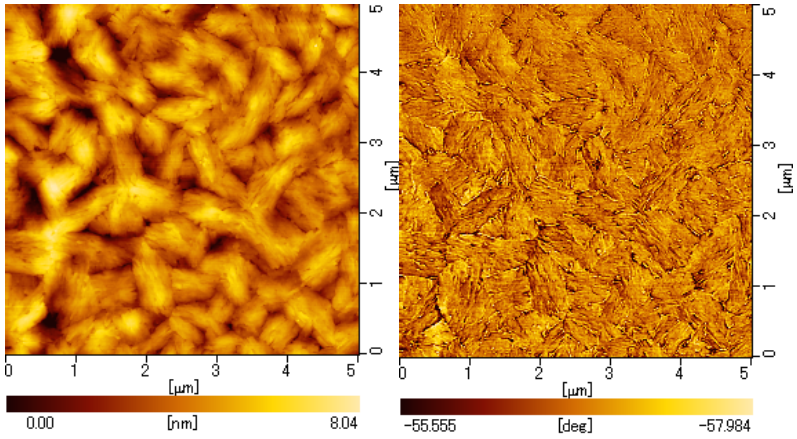

b)

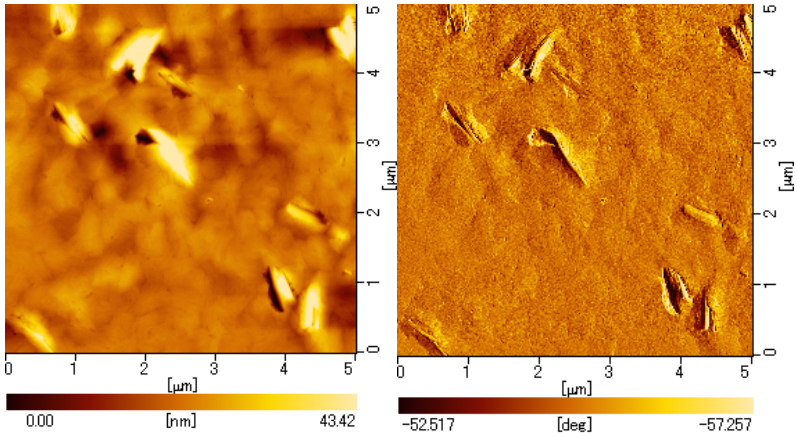

Fig. S15 Tapping–mode AFM height (left) and phase (right) images of **PCBM**-layers on p-i–layer with a) **BP–C_{60}** for i-layer and b) **BP:PCBM** for i-layer. RMS values are 1.23 and 6.42 nm for a) and b).

8. XRD

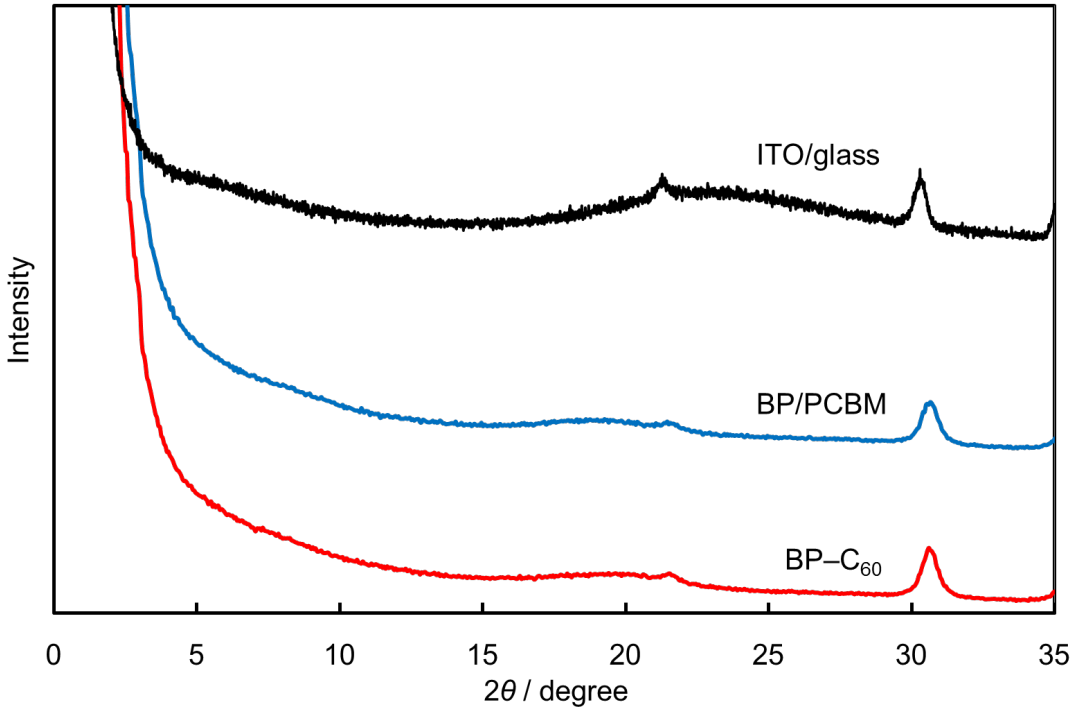

Fig. S16 Out-of-plane XRD patterns of **BP–C_{60}** layer and **BP/PCBM** layer on top of glass/ITO/PEDOT:PSS.

6. Characterization of compounds

^{1}H NMR spectrum ($CDCl_3$) of **4**

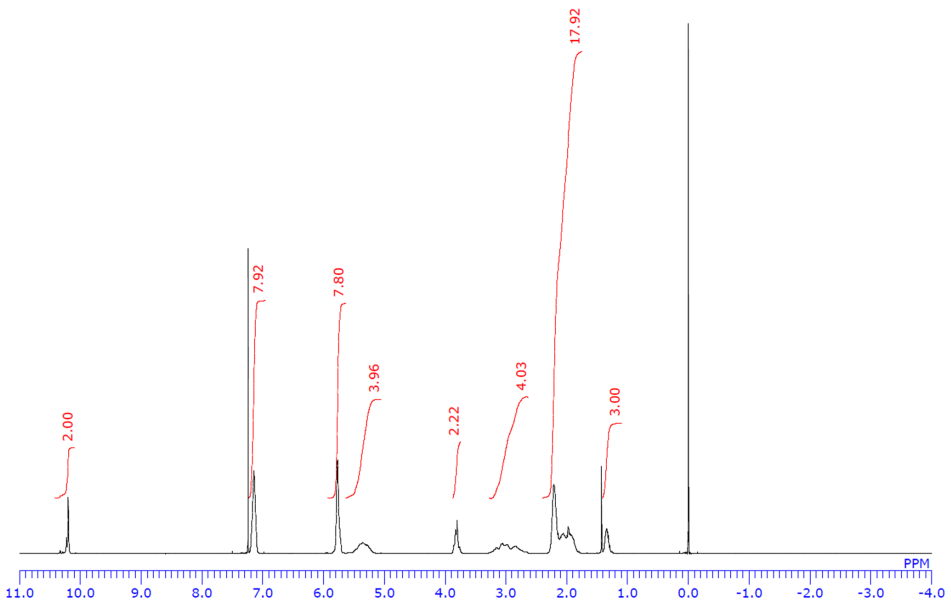

^{13}C NMR spectrum ($CDCl_3$) of **4**. (Minor peaks are occasionally observed alongside of the main peaks, which are presumably from the structural isomers differing in the orientation of bicycle[2.2.2]octadieno-units. The minor peaks are also listed in the spectroscopic characterization data above.)

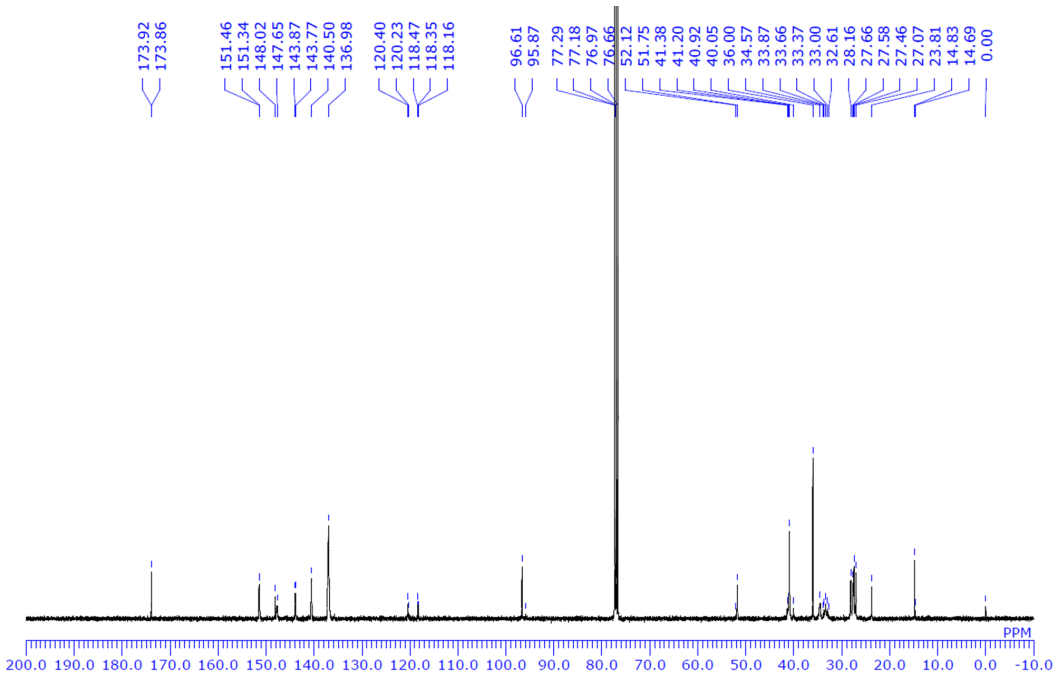

^{13}C NMR spectrum ($CDCl_3$) of **4** (0.0–60 ppm).

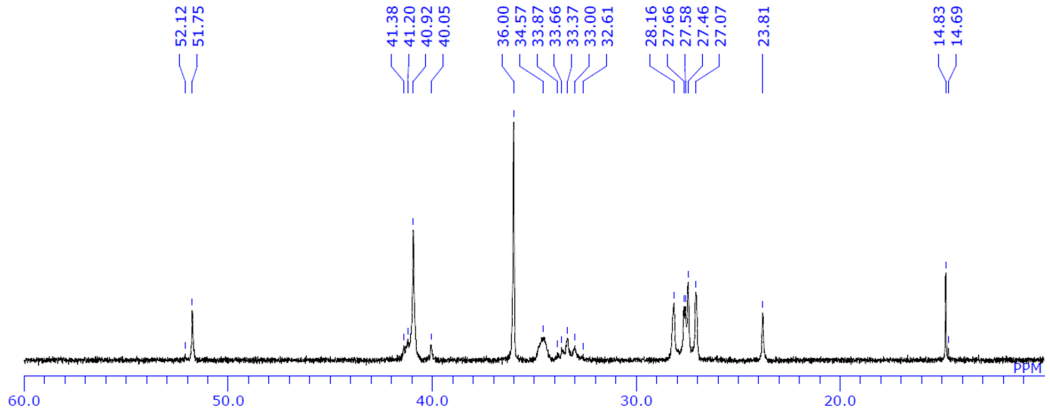

^{13}C NMR spectrum ($CDCl_3$) of **4** (90.0–130.0 ppm)

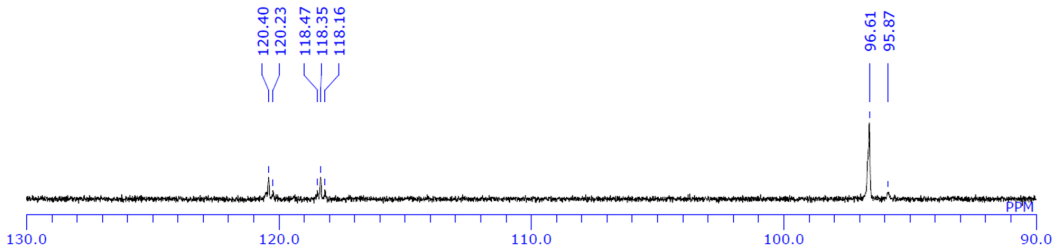

^{13}C NMR spectrum ($CDCl_3$) of **4** (130.0–180.0 ppm)

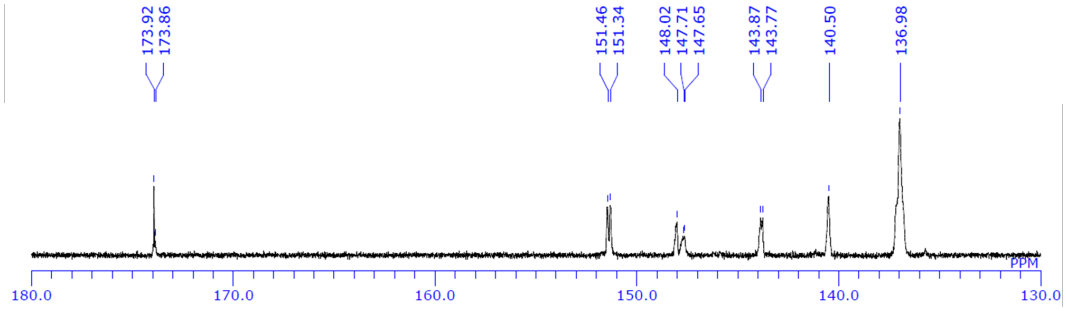

^{1}H NMR spectrum ($CDCl_3$) of **5**

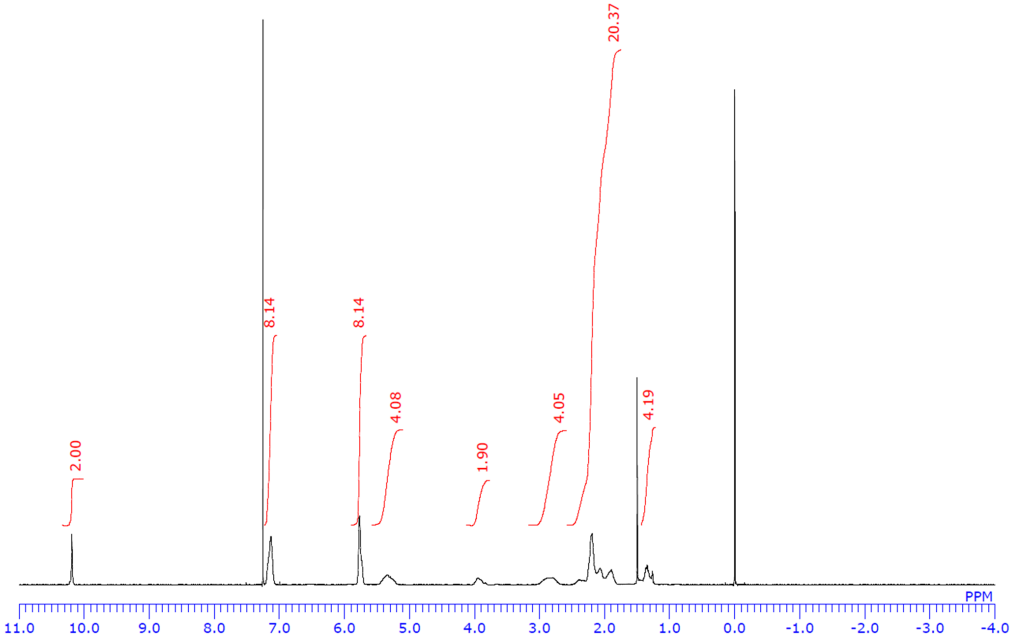

^{13}C NMR spectrum ($CDCl_3$) of **5**. (Minor peaks are occasionally observed alongside of the main peaks, which are presumably from the structural isomers differing in the orientation of bicycle[2.2.2]octadieno-units. The minor peaks are also listed in the spectroscopic characterization data above.)

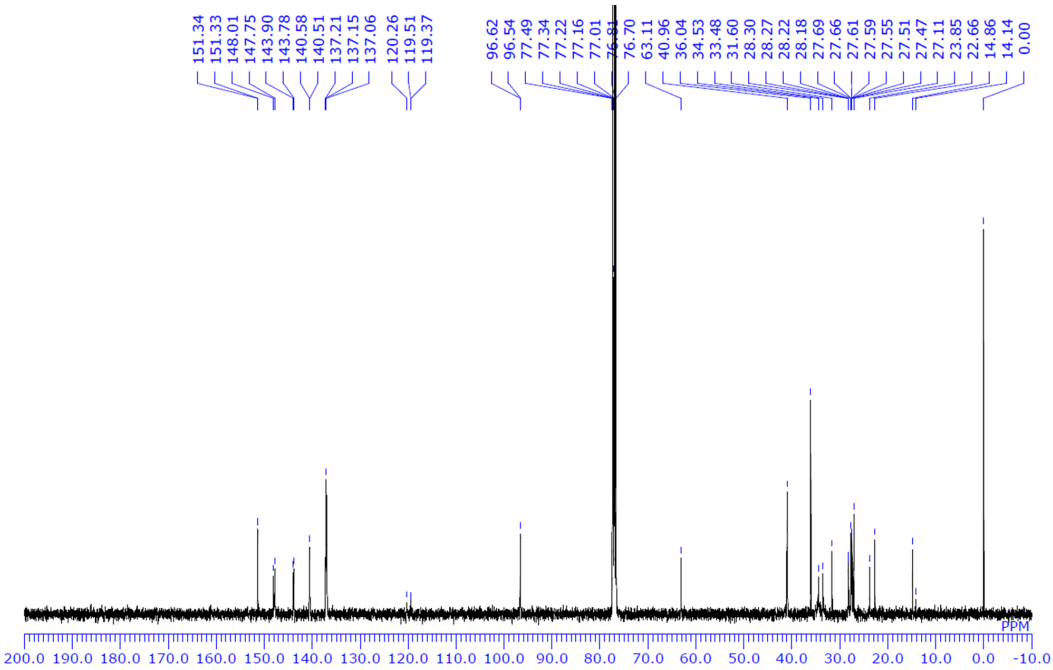

^{13}C NMR spectrum ($CDCl_3$) of **5** (0.0–70 ppm)

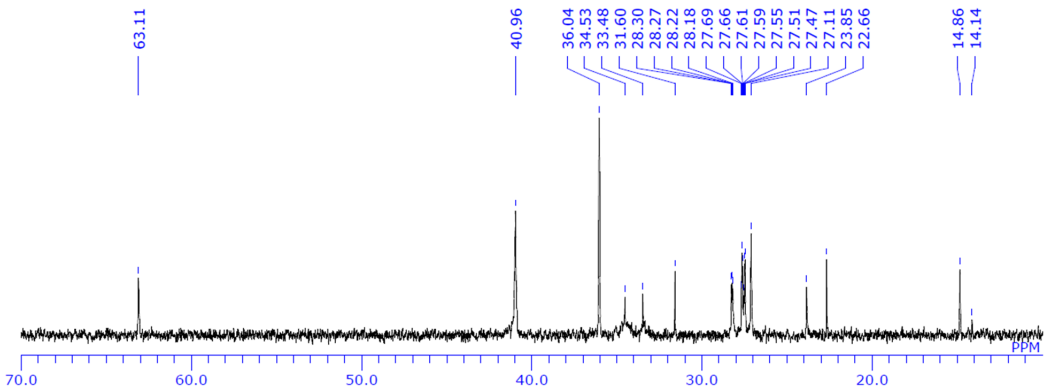

^{13}C NMR spectrum ($CDCl_3$) of **5** (0.0–70 ppm)

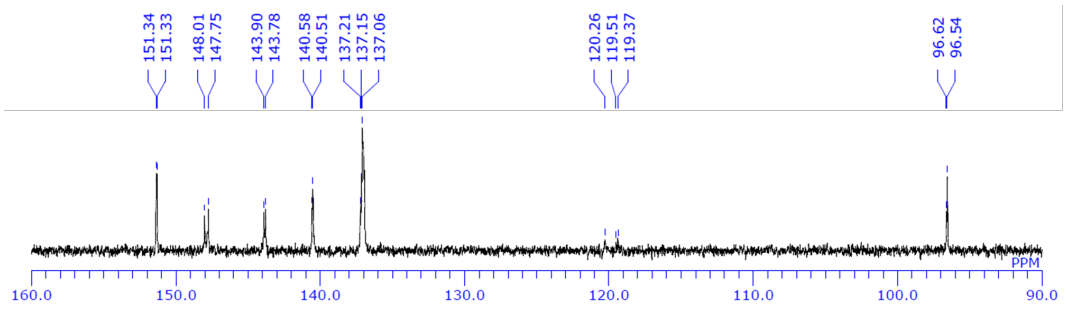

^{1}H NMR spectrum ($CDCl_3$) of **ZnCP-C$_{60}$**

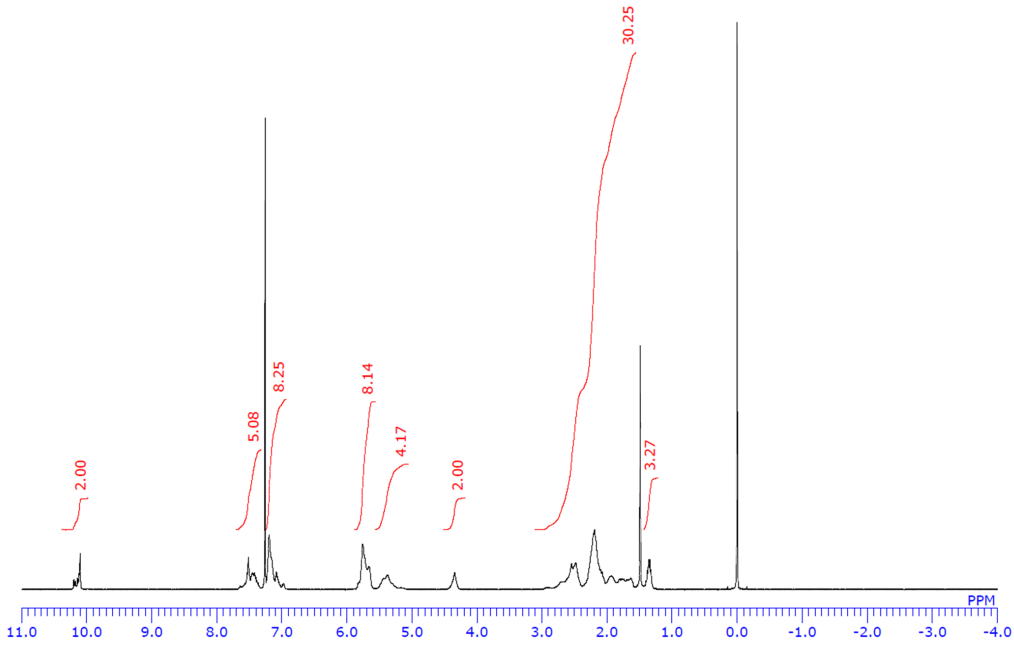

^{13}C NMR spectrum ($CDCl_3$) of **ZnCP-C$_{60}$**. (Minor peaks and peak broadening are observed, presumably because of the intra- or intermolecular interactions between the C60 core and the porphyrin unit, associated with the existence of structural isomers differing in the orientation of bicycle[2.2.2]octadieno-units. The minor peaks are also listed in the spectroscopic characterization data above.)

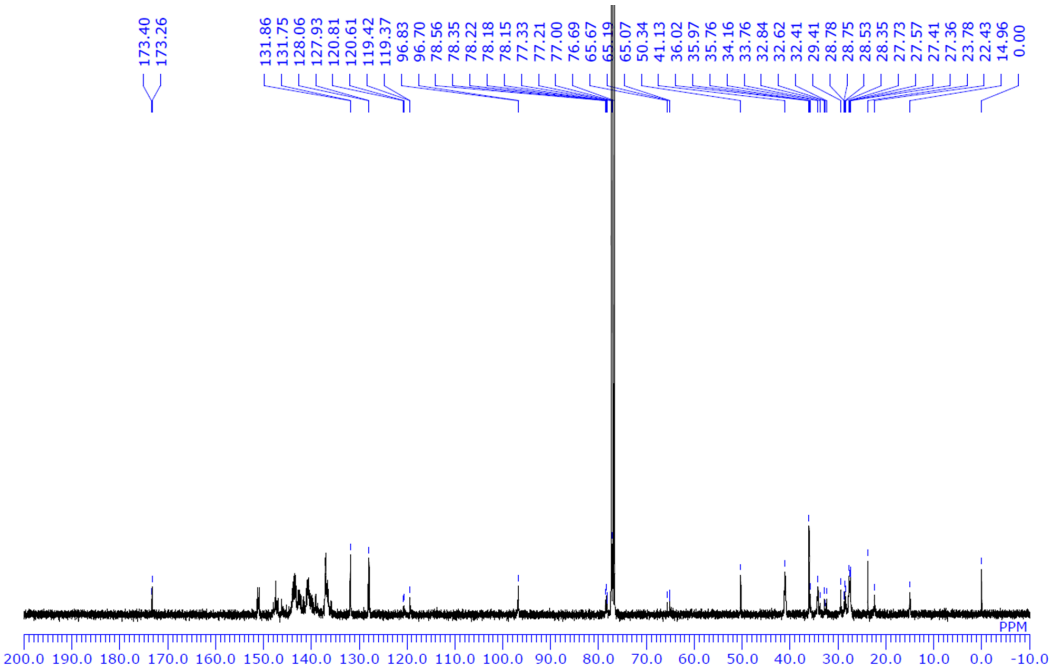

^{13}C NMR spectrum ($CDCl_3$) of **ZnCP-C$_{60}$** (10.0–70.0 ppm)

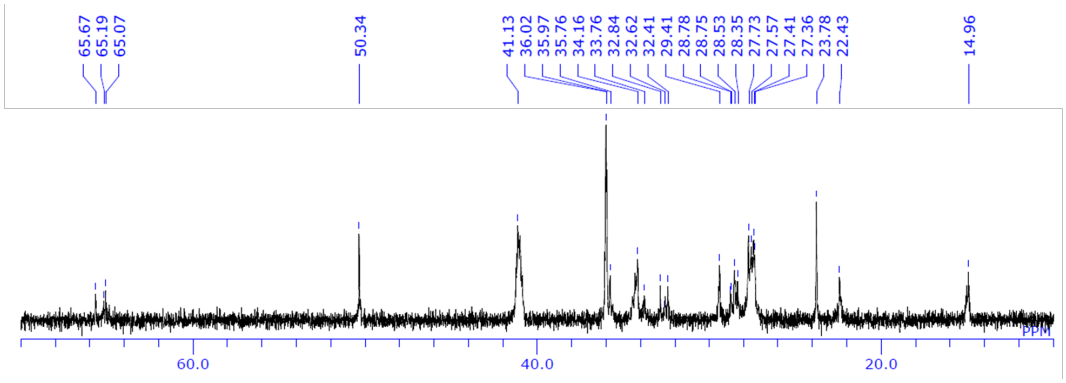

^{13}C NMR spectrum ($CDCl_3$) of **ZnCP-C$_{60}$** (75.0–125.0 ppm)

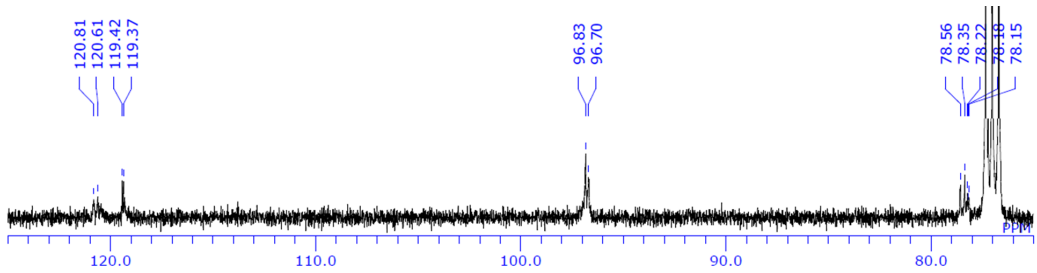

^{13}C NMR spectrum ($CDCl_3$) of **ZnCP-C$_{60}$** (125.0–180.0 ppm)

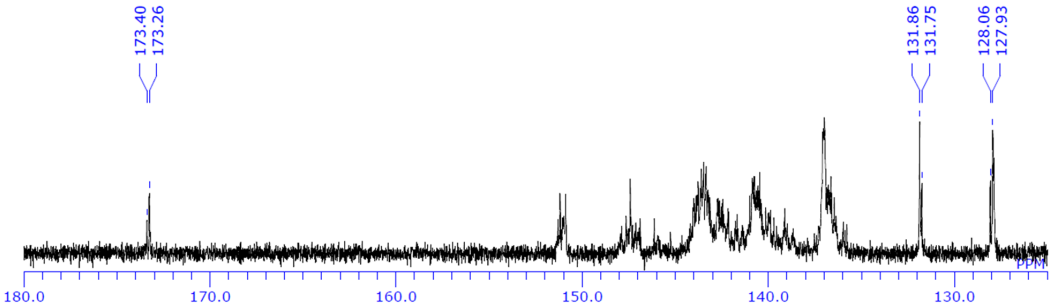

^{1}H NMR spectrum ($CDCl_3$) of **CP-C$_{60}$**

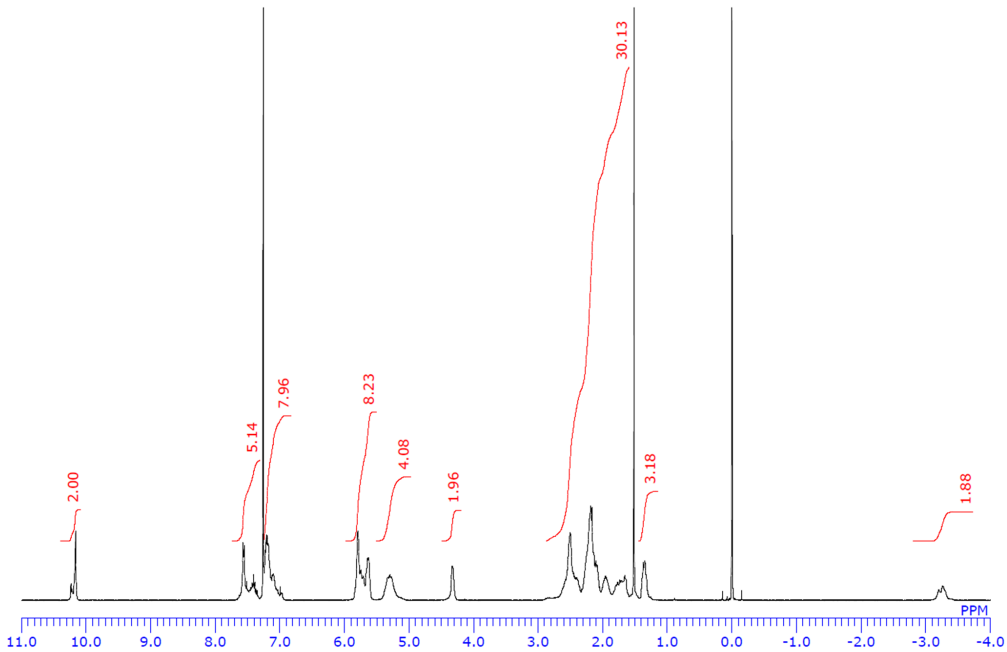

^{13}C NMR spectrum ($CDCl_3$) of **CP-C$_{60}$**. (Minor peaks and peak broadening are observed, presumably because of the intra- or intermolecular interactions between the C60 core and the porphyrin unit, associated with the existence of structural isomers differing in the orientation of bicycle[2.2.2]octadieno-units. The minor peaks are also listed in the spectroscopic characterization data above.)

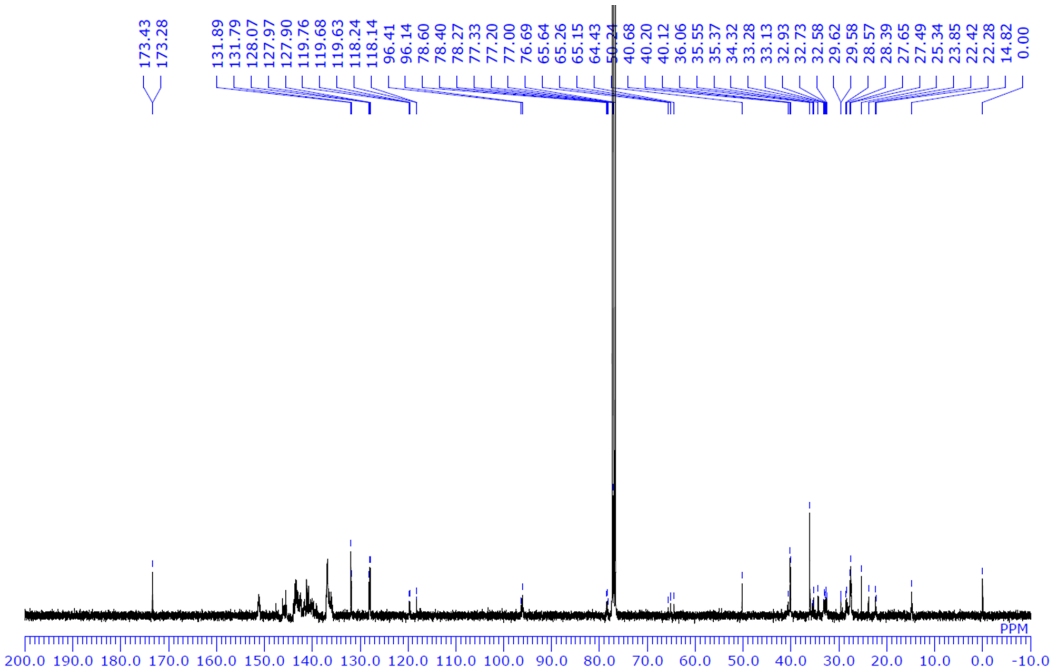

^{13}C NMR spectrum ($CDCl_3$) of **CP-C$_{60}$** (10.0–70.0 ppm)

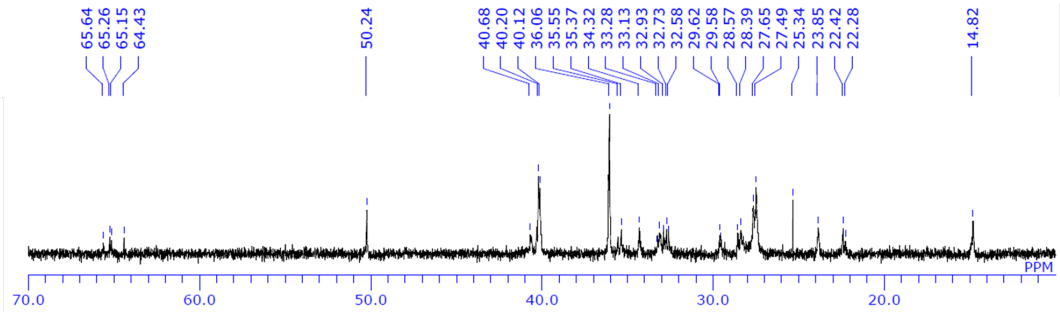

^{13}C NMR spectrum ($CDCl_3$) of **CP-C$_{60}$** (75.0–125.0 ppm)

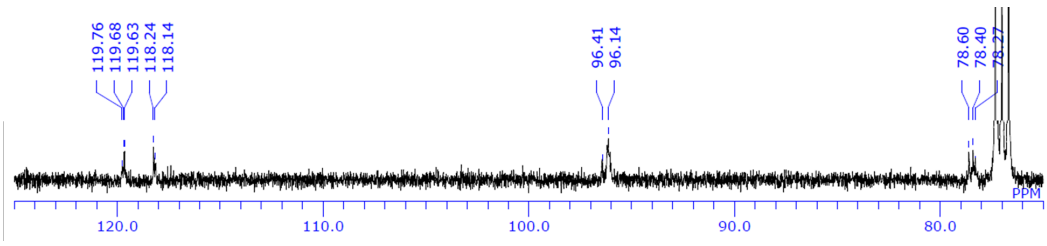

^{13}C NMR spectrum ($CDCl_3$) of **CP-C$_{60}$** (125.0–180.0 ppm)

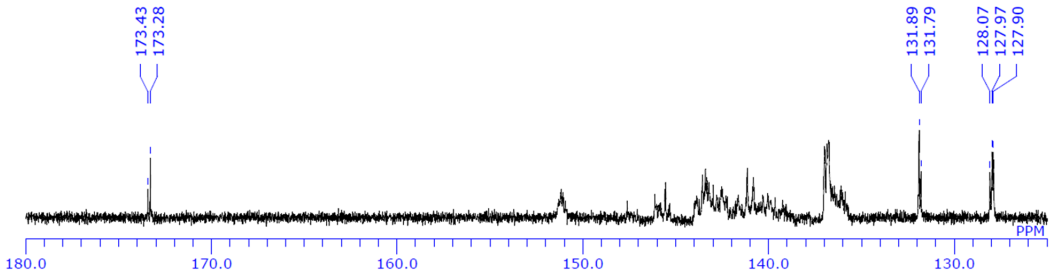

^{1}H NMR spectrum ($CDCl_3$) of **BuCP**

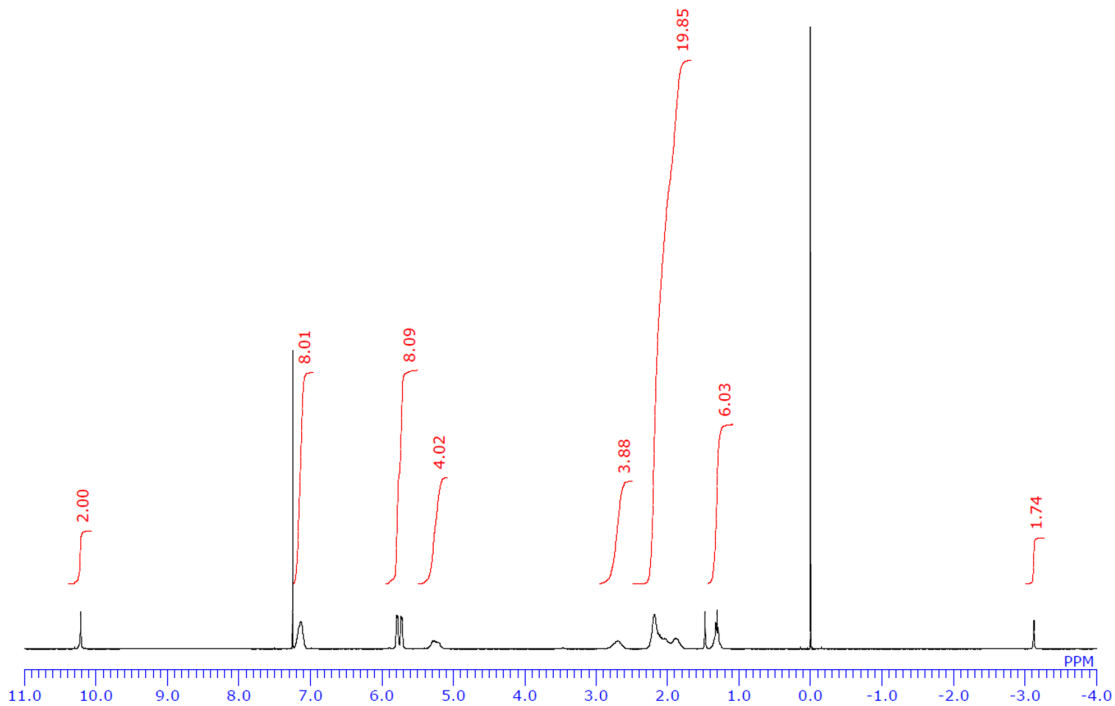

^{13}C NMR spectrum ($CDCl_3$) of **BuCP**. (Minor peaks are occasionally observed alongside of the main peaks, which are presumably from the structural isomers differing in the orientation of bicycle[2.2.2]octadieno-units. The minor peaks are also listed in the spectroscopic characterization data above.)

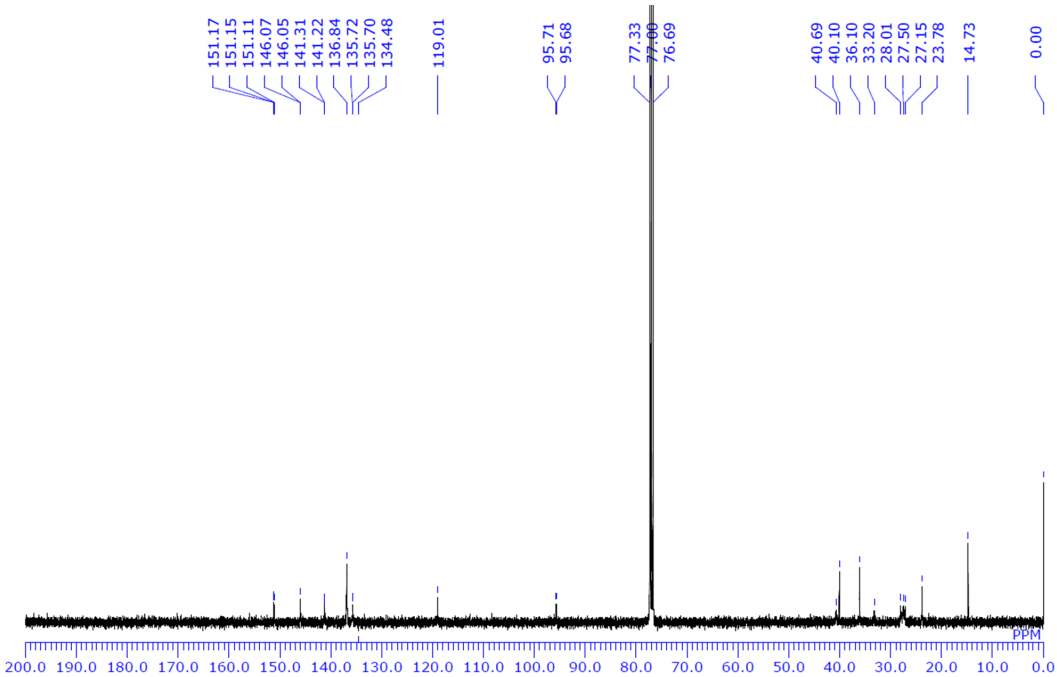

^{13}C NMR spectrum ($CDCl_3$) of **BuCP** (0.0–50.0 ppm)

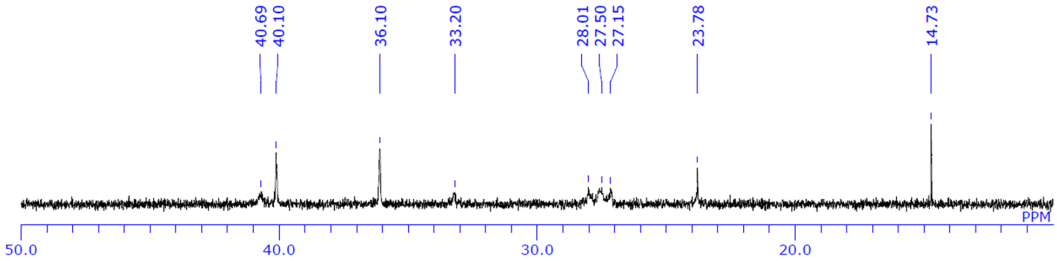

^{13}C NMR spectrum ($CDCl_3$) of **BuCP** (90–125 ppm)

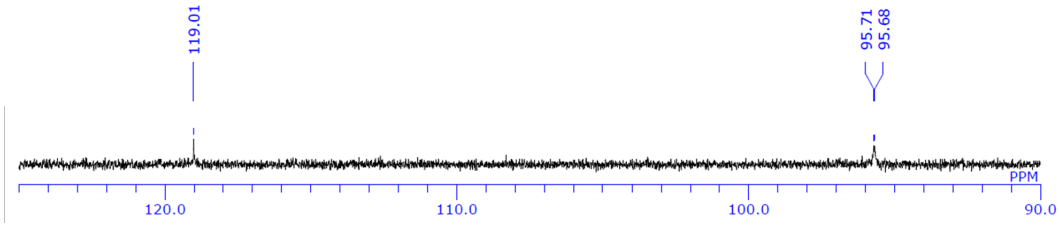

^{13}C NMR spectrum ($CDCl_3$) of **BuCP** (130–160 ppm)

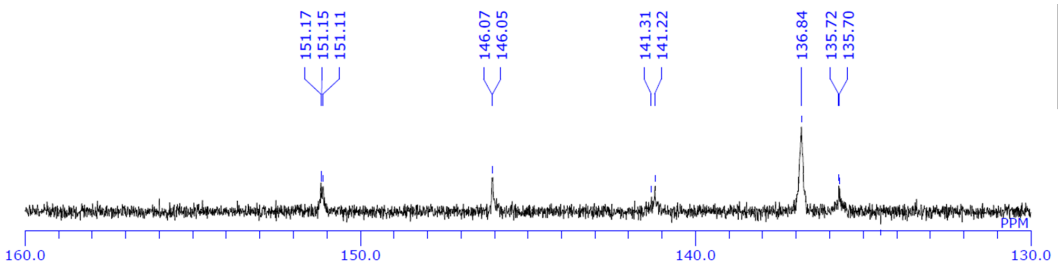

Reference

1. H. Yamada, K. Kishibe, T. Okujima, H. Uno, N. Ono, *Chem Commun.*, 2006, 383-385
2. V. Hickmann, A. Kondoh, B. Gabor, M. Alcarazo and A. Fürstner, *J. Am. Chem. Soc.* 2011, **133**, 13471.
3. T. Nishizawa, K. Tajima, K. Hashimoto, *J. Mater. Chem.*, 2007, **17**, 2440-2445